The EMBO Journal (2009) 28, 1099–1110 | © 2009 European Molecular Biology Organization | All Rights Reserved 0261-4189/09
www.embojournal.org

THE EMBO JOURNAL

Mimicking Ndc80 phosphorylation triggers spindle assembly checkpoint signalling

Stefan Kemmler[1,3], Manuel Stach[1], Maria Knapp[1], Jennifer Ortiz[1], Jens Pfannstiel[1,4], Thomas Ruppert[2] and Johannes Lechner[1,*]

[1]Biochemie-Zentrum der Universität Heidelberg, Im Neuenheimer Feld 328, Heidelberg, Germany and [2]Zentrum für Molekulare Biologie, Im Neuenheimer Feld 282, Heidelberg, Germany

The protein kinase Mps1 is, among others, essential for the spindle assembly checkpoint (SAC). We found that *Saccharomyces cerevisiae* Mps1 interacts physically with the N-terminal domain of Ndc80 ($Ndc80^{1-257}$), a constituent of the Ndc80 kinetochore complex. Furthermore, Mps1 effectively phosphorylates $Ndc80^{1-257}$ *in vitro* and facilitates Ndc80 phosphorylation *in vivo*. Mutating 14 of the phosphorylation sites to alanine results in compromised checkpoint signalling upon nocodazole treatment of mutants. Mutating the identical sites to aspartate (to simulate constitutive phosphorylation) causes a metaphase arrest with wild-type-like bipolar kinetochore–microtubule attachment. This arrest is due to a constitutively active SAC and consequently the inviable aspartate mutant can be rescued by disrupting SAC signalling. Therefore, we conclude that a putative Mps1-dependent phosphorylation of Ndc80 is important for SAC activation at kinetochores.

The EMBO Journal (2009) **28,** 1099–1110. doi:10.1038/emboj.2009.62; Published online 19 March 2009
Subject Categories: signal transduction; cell cycle
Keywords: centromere; kinetochore; Mps1; Ndc80; spindle assembly checkpoint

Introduction

Accurate chromosome segregation requires that sister kinetochores attach to microtubules emanating from opposing poles (bipolar attachment) before sister chromatides separate. This mitotic dependency is supervised by the spindle assembly checkpoint (SAC) in eukaryotic cells (Musacchio and Salmon, 2007). In *Saccharomyces cerevisiae*, the SAC signal is executed by the SAC components Mad1, Mad2, Mad3, Bub1, Bub3 and Mps1 that localize to kinetochores lacking bipolar attachment (Gillett *et al*, 2004; Vigneron *et al*, 2004; Chan *et al*, 2005) and cooperate in inactivating the anaphase promoting complex (APC) through its regulatory subunit Cdc20 (Musacchio and Salmon, 2007). As APC is required to mark Pds1/Securin, an inhibitor of the cohesion-cutting protease Esp1/Separin, for degradation, an activated SAC prevents sister chromatid separation until all sister kinetochores have obtained a bipolar attachment. The SAC machinery recognizes kinetochores that have not achieved bipolar attachment either because these kinetochores are not attached to microtubules and/or because they lack the appropriate tension. In *S. cerevisiae*, the Ipl1/Sli15/Bir1 complex has been proposed to serve as the tension sensor (Sandall *et al*, 2006). Also, Ipl1 has been suggested to translate missing tension into nonattached kinetochores (Biggins and Murray, 2001; Tanaka *et al*, 2002) possibly by phosphorylating subunits of the Dam1 complex (Cheeseman *et al*, 2002), which contributes to the kinetochore–microtubule interface in *S. cerevisiae*. This would make nonattached kinetochores the predominant direct origin of SAC activation.

Mps1 is the only essential SAC protein in *S. cerevisiae* because Mps1 has additional cellular roles, besides SAC function. In *S. cerevisiae*, these include spindle pole body duplication (Winey *et al*, 1991) and the regulation of kinetochore–microtubule interaction (Jones *et al*, 2005; Shimogawa *et al*, 2006). SAC function of Mps1 has been demonstrated in *S. cerevisiae* by *mps1* mutant analysis (Weiss and Winey, 1996) and by Mps1 overexpression (Hardwick *et al*, 1996). The latter induces a constitutive checkpoint arrest that is dependent on the remaining SAC components. Beside its general SAC function, Mps1 facilitates SAC activation as a result of lacking tension at the kinetochores (Maure *et al*, 2007; Jelluma *et al*, 2008). In *Xenopus*, kinetochore localization of Mps1 depends on the Ipl1/AuroraB-Sli15/Survivin-Bir1/INCENP complex and Bub1 (Vigneron *et al*, 2004). Conversely, the kinetochore localization of Bub1 as well as Mad1 and Mad2 depends on Mps1 in this system, which may indicate that Mps1 is targeting SAC components to kinetochores. However, with the exception of Mad1 (Hardwick *et al*, 1996), and Borealin in mammals (Jelluma *et al*, 2008), no substrate of the Mps1 kinase that functions in the context of SAC activation has been described to date.

How kinetochores contribute to SAC activation is poorly understood. The presence of polo kinase-dependent phosphoepitopes (3F3/2 epitopes) at vertebrate kinetochores strongly correlates with the absence of tension (Nicklas *et al*, 1995; Ahonen *et al*, 2005; Wong and Fang, 2005). Furthermore, polo kinase targets Mad2 and BubR1 (the vertebrate Mad3 homologue) to *Xenopus* kinetochores and may contribute to target Mad2 to mammalian kinetochores (Wong and Fang, 2005). However, the kinetochore components that harbour the 3F3/2 epitopes have not been identified to date. Also, the kinetochore proteins that directly contribute to the kinetochore binding of the SAC components have not been elucidated yet. On the other side, it has been

*Corresponding author. Biochemie-Zentrum der Universität Heidelberg, Ruprecht-Karls-Universität, Im Neuenheimer Feld 328, Raum 208, Heidelberg, BW 69120, Germany. Tel.: +49 6221 544371; Fax: +49 6221 544790; E-mail: johannes.lechner@bzh.uni-heidelberg.de
[3]Present address: Institute of Biochemistry, ETH Zürich, Schafmattstr. 18, Zürich 8093, Switzerland
[4]Present address: Universität Hohenheim, Institut für Physiologie 230c, Stuttgart 75099, Germany

Received: 26 August 2008; accepted: 18 February 2009; published online: 19 March 2009

shown that SAC function and kinetochore targeting of SAC components is dependent on the Ndc80 complex (Janke *et al*, 2001; Martin-Lluesma *et al*, 2002; DeLuca *et al*, 2003; McCleland *et al*, 2003; Gillett *et al*, 2004), a conserved kinetochore component that contributes to the microtubule-binding interface of kinetochores (Cheeseman *et al*, 2006; DeLuca *et al*, 2006). In *S. cerevisiae*, similar to mammalian cells, the subunits Ndc80 and Nuf2 as well as Spc24 and Spc25 form heterodimers, respectively (Ciferri *et al*, 2005; Wei *et al*, 2005, 2007). These dimers are held together by coiled-coil interactions and associate with each other tail-to-tail to form a heterotetramer. The Ndc80 complex thus appears as a long rod with two globular domains on each side (one for each subunit). The globular domains of Spc24 and Spc25 are oriented to the inner kinetochore, and the globular domains of Ndc80 and Nuf2 are oriented to the outer kinetochore (Wei *et al*, 2005). The latter two represent calponin-homology domains (Wei *et al*, 2007; Ciferri *et al*, 2008). Basic residues within these domains and possibly within the N-terminal unstructured region of Ndc80 are important for microtubule binding of the Ndc80 complex (Ciferri *et al*, 2008).

Here, we show that Mps1 phosphorylates Ndc80 *in vitro* and facilitates Ndc80 phosphorylation *in vivo*. Mutating sufficient phosphorylation sites to alanine compromises SAC function. Mutating the same sites to aspartate causes a constitutive SAC activation although kinetochore-spindle attachment is stable enough to produce tension at the kinetochores and to support cell viability when SAC signalling is disrupted.

Results

Mps1 physically interacts with the N-terminal domain of Ndc80

When we isolated the Ndc80 complex using Protein A-tagged Spc24, we found small amounts of co-purifying Mps1 (Figure 1A), and upon Mps1 overexpression, the amount of co-purifying Mps1 markedly increased (Figure 1B). We speculated that Mps1 might interact with Ndc80 complex components that contribute to the microtubule interface and therefore co-expressed a 10His-Ndc80/Nuf2 heterodimer together with Mps1 in *Escherichia coli*. Affinity purification of 10His-Ndc80 revealed a physical interaction of Mps1 with the 10His-Ndc80/Nuf2 heterodimer and/or 10His-Ndc80 *per se* (Figure 1C). As mentioned earlier, Ndc80 and Nuf2 consist of C-terminal coiled-coil regions that confer interactions within the Ndc80 complex and of N-terminal globular domains. We speculated that the latter might interact with Mps1. When Mps1 was co-expressed with the His-tagged N-terminal domain of Ndc80 ($Ndc80^{1-257}$) or Nuf2 ($Nuf2^{1-219}$), only interaction of Mps1 with the former was detected (Figure 1C and not shown). Therefore, we conclude that Mps1 interacts specifically with the N-terminal domain of Ndc80. Mps1 localization at metazoan kinetochores has been described (see 'Introduction'). Also, evidence for the localization at *S. cerevisiae* kinetochores exists (Castillo *et al*, 2002; Maure *et al*, 2007). We confirmed this point by chromatin immunoprecipitation (ChIP) with Mps1-9Myc (Figure 1D). Therefore, Mps1 may localize to the *S. cerevisiae* kinetochore through the N-terminal domain of Ndc80.

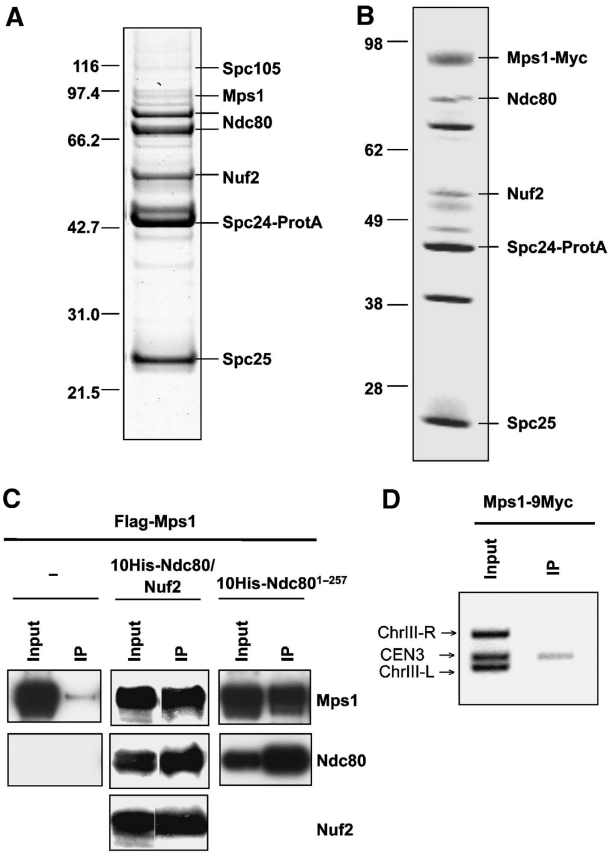

Figure 1 Mps1 physically interacts with Ndc80 and localizes to the kinetochore. (**A**) The Ndc80 complex was purified through protein A-tagged Spc24 by affinity chromatography with IgG-sepharose and fractionated by SDS–PAGE. Proteins were identified from Coomassie-stained bands by peptide mass fingerprinting (MALDI-TOF). Bands that are not labelled represent contaminants. (**B**) As in (A) with the exception that the Ndc80 complex was purified from cells overexpressing Mps1 (strain YSK632). (**C**) Mps1 and Ndc80 interact *in vitro*. Flag-Mps1, 10His-$Ndc80^{1-257}$ or 10His-Ndc80 and Nuf2 were co-expressed in *E. coli* as indicated. 10His-Ndc80 or 10His-$Ndc80^{1-257}$ was affinity purified with NTA-agarose (IP). Input (0.01% of total) and IP (1% of total) were subjected to western analysis with anti-Flag, anti-His and anti-Nuf2 antibodies. (**D**) ChIP analysis. Mps1-9Myc was immunoprecipitated with anti-Myc antibody. The presence of *CEN3* DNA and two flanking DNA regions (ChIII-R and ChIII-L) was analysed by PCR in the input and the immunoprecipitate (IP).

Mps1 phosphorylates Ndc80 in vitro and supports Ndc80 phosphorylation in vivo

As Mps1 interacts with the Ndc80 complex, we tested whether the Ndc80 complex is a substrate of Mps1. *In vitro* kinase assays with the purified Ndc80 complex and Mps1 purified from *S. cerevisiae* revealed strong autophosphorylation of Mps1 and that Mps1 phosphorylates Ndc80 efficiently (Figure 2A). Nuf2, Spc24 and Spc25 phosphorylation was considerably less prominent. Furthermore, we found that $Ndc80^{1-257}$ purified from *E. coli* serves as a very good Mps1 substrate in the *in vitro* assay (Figure 2B). This is in agreement with the finding that Mps1 interacts with $Ndc80^{1-257}$ *in vitro*. As mentioned earlier, Mps1 overexpression results in a constitutive activation of the SAC in *S. cerevisiae*. Therefore, we asked whether Mps1 overexpression results in hyperphosphorylated Ndc80. Indeed, after Mps1 overexpression,

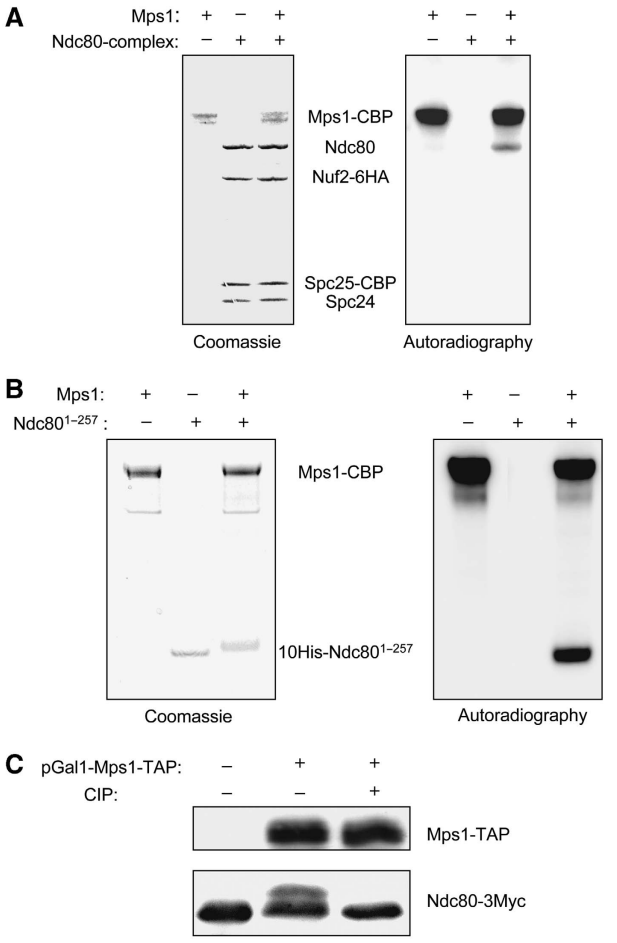

Figure 2 Mps1 phosphorylates Ndc80. (**A**) *In vitro* kinase assay. The Ndc80 complex and Mps1 were individually purified from *S. cerevisiae* by tandem affinity purification and incubated with γ-^{32}P-ATP as indicated. Samples were fractionated by SDS–PAGE and visualized by Coomassie staining plus autoradiography as indicated. CBP, calmodulin-binding peptide. (**B**) As in (A) with the exception that the His-tagged N-terminal domain of Ndc80 (10His-Ndc80$^{1-257}$) purified from *E. coli* was used instead of the Ndc80 complex. (**C**) Mps1 facilitates Ndc80 phosphorylation *in vivo*. Whole cell extracts were subjected to western analysis with peroxidase-anti-peroxidase (to detect Mps1-TAP) and anti-Myc antibody (to detect Ndc80-3Myc). As shown, control cells (YSK658: *NDC80-3MYC*) or cells overexpressing Mps1-TAP (YSK658 harbouring plasmid pSK950: *pGAL1-MPS1-TAP, 2* μ) were analysed. Extracts were treated with 10 U calf intestinal phosphatase (CIP) for 1 h at 30°C as indicated.

a lower-mobility form of Ndc80 could be detected by SDS–PAGE (Figure 2C). Phosphatase treatment reverted this form's mobility back to the original. Thus, Mps1 overexpression results in Ndc80 hyperphosphorylation.

Analysis of Ndc80 phosphorylation sites

To identify Mps1-dependent phosphorylation sites, we performed *in vitro* phosphorylation of purified Ndc80$^{1-257}$, subjected it to in-gel digestion with trypsin and analysed phosphopeptides by LC-ESI-MS/MS (see Materials and methods). This identified at least 25 phosphorylated sites in Ndc80$^{1-257}$ (Table I). To compare *in vivo* and *in vitro* Mps1-dependent phosphorylation of Ndc80, we purified the Ndc80 complex from cells that overexpressed Mps1 for 3 h,

Table I Ndc80$^{1-257}$ phosphorylation sites

Amino acids	Peptides identified	Maximal number of phosphates detected together on the peptide	
		In vitro	*In vivo*
1–19	MQ***SSTST***DQHVLHHMDPHR	2	2
20–33	F***TS***QIP**T**A**T**SSQLR	3	1
36–52	N***ST***NQGL**T**DMINK**S**IAR	3	2
53–67	N**T**I**S**G**T**GIP**T**GGINK	3	2
73–89	***ST***VAGG**T**NG**T**ALALNDK**S**NSR	3	—
94–114	NSV**S**RL**S**INQLG**S**LQQHLSNR	3	1
121–137	DKNFQ***S***AIQEEIYDYLK	1	—
141–152	FDIE**T**NHPI**S**IK	2	—
173–181	LDPGYGF**T**K	1	—
205–217	**S**QISAVGGSNWHK	1	—
242–257	SLINQN**T**QEI**T**ILSQP	2	2

Sites were identified by mass spectrometry as described in the text.
Sites detected *in vitro* are indicated in bold.
Sites detected *in vitro* and *in vivo* are bold underlined.
Unresolved which of the neighbouring sites is phosphorylated are indicated in italics.

subjected Ndc80 to in-gel digestion with trypsin and analysed phosphopeptides by LC-ESI-MS/MS. Ten phosphorylated sites were detected in the N-terminal domain of Ndc80 (Table I). All of these sites had been identified by the *in vitro* approach. In addition, one site at the very C-terminus (T690) was detected. The fact that several sites found *in vitro* were not detected *in vivo* might reflect altered accessibility of sites by Mps1 *in vivo* versus *in vitro*. Alternatively, some phosphorylation sites were not detectable, because we subjected about five times less *in vivo* material than *in vitro* material to mass spectrometry. Two of the phosphorylated residues (S100 and T248) were also detected when Ndc80 from control cells (without Mps1 overexpression) was analysed. This may be the result of endogenous Mps1 activity. For S100, it may be also due to Ipl1 activity, as this residue is part of an Ipl1 consensus site (Cheeseman *et al*, 2002). All phosphorylated amino acids were either serines or threonines. No phosphorylated tyrosine was detected, although Mps1 has been described as a dual specific kinase (Lauze *et al*, 1995). In some cases, the MS/MS fragmentation pattern only allowed to attribute a phosphate group to either of two or more neighbouring serines and threonines (Table I). Frequently multiple phosphorylated peptides were observed (Table I), indicating that many of the identified phosphorylated residues occur together on the same Ndc80 molecule. According to the structural data provided recently for the human Ndc80 N-terminal domain (Wei *et al*, 2007) and for the human Ndc80-Nuf2 heterodimer (Ciferri *et al*, 2008), the Ndc80 N-terminus consists of an unstructured N-terminal tail followed by a six-helix calponin-homology domain. On the basis of sequence and structure alignments between human and *S. cerevisiae* Ndc80 (Wei *et al*, 2007), 18 of the identified phosphorylation sites reside in the unstructured N-terminal tail of *S. cerevisiae* Ndc80 (amino acids 1–113), one site (S126) corresponds to α helix 1, one (S205) to α helix 5, two to loop 1/2, one to loop 3/4 and two are in the sequence that links α helix 6 with the coiled-coil region (Supplementary Figure S1). With the exception of S205 and to a lesser extent S150 and maybe S4 and T5, the identified sites are not conserved between *S. cerevisiae* and higher eukaryotes.

Table II Ndc80 phosphorylation sites mutated to alanine

Mutations	Drug[a] sensitive	Mutant
S205A	–	
S205A T248A T252A	–	*ndc80-3A*
S37A T38A T43A S205A T248A T252A	–	*ndc80-6A*
T21A S22A S37A T38A T43A S205A T248A T252A	–	*ndc80-8A*
S4A T5A S6A T21A S22A S37A T38A T43A S205A T248A T252A	+	*ndc80-11A*
S4A T5A S6A T21A S22A S37A T38A T43A T74 T79 T82 S205A T248A T252A	+	*ndc80-14A*
S4A T5A S6A T21A S22A S37A T38A T43A	–	
S4A T5A S6A T21A S22A S37A T38A T43A T145A S150A S205A	–	*ndc80-11A**
T145A S150A S205A	–	
T145A S150A S205A T248A T252A T255A	–	

[a]Benomyl or nocodazole.

Mutating Ndc80 phosphorylation sites to alanine results in a compromised SAC

The high number of phosphorylation sites identified made a complete analysis of all possible mutant combinations not feasible. Thus, our initial strategy was to mutate increasing numbers of corresponding serine and threonine residues to alanine and test for benomyl sensitivity as a first indicator for a SAC defect. For technical reasons, we mutated sites in close proximity together. Also, in two cases where it was unclear, which of two neighbouring sites (T21 versus S22 and S37 versus T38) was the phosphorylated one (see above), we mutated both. In the region S2–S6, where two phosphate residues had been identified, we mutated three sites. Of the mutant combinations tested, strains with $\leqslant 8$ mutations were not benomyl sensitive (Figure 3A; Table II). However, a strain with 11 mutations (*ndc80-11A*) exhibited clear benomyl sensitivity (Figure 3A; Table II). Notably, strain *ndc80-11A** that also carries 11 mutations but has T145A and S150A instead of T248A and T252A (as in *ndc80-11A)* was not benomyl sensitive. Thus, the T248A and T252A mutations contributed strongly to the benomyl sensitive phenotype. Mutating 14 phosphorylation sites to alanine (*ndc80-14A*) also caused benomyl sensitivity (Figure 3A). Furthermore, it severely decreased cell viability when cells were incubated with nocodazole (Figure 3B; Table II), providing further evidence that eliminating sufficient phosphorylation sites can compromise SAC function. To support this, we released α factor arrested wild-type and *ndc80-14A* cells into nocodazole and analysed Pds1 degradation kinetics. As expected, both strains increased Pds1 levels initially. However, whereas wild-type cells maintain high Pds1 levels due to the APC inactivation by SAC, the Pds1 level in *ndc80-14A* decreased markedly throughout the nocodazole arrest (Figure 3C and D). This is in agreement with a compromised SAC function in *ndc80-14A* cells.

Mutating Ndc80 phosphorylation sites to aspartate causes constitutive SAC activation

If elimination of phosphorylation sites results in SAC defects, simulating constitutive phosphorylation by serine/threonine to aspartate mutations might cause aberrant SAC activation. Corresponding to *ndc80-11A* and *ndc80-14A*, we constructed the aspartate mutants *ndc80-11D* and *ndc80-14D*. When tested for growth on benomyl plates, *ndc80-11D* surprisingly not only lacked the benomyl sensitivity of *ndc80-11A* but was considerably more resistant to benomyl than wild-type cells (Figure 4A). This indicated that simulating constitutive phosphorylation as *in ndc80-11D* might enhance SAC activation and thus allow the cells to cope with microtubule stability interferences better than wild-type cells. If the introduction of 11 aspartates enhances SAC activation, then mutating further sites to aspartate might cause permanent SAC activation and consequently cell death. Indeed, *ndc80-14D*, in contrast to *ndc80-14A*, was dead (Figure 7A, lane 2). Already the overexpression of wild-type Ndc80 resulted in very sick cells. Therefore, overexpression of Ndc80-14D was not a feasible option to determine the arrest phenotype of *ndc80-14D*. Instead, we constructed a strain that expressed a destabilized wild-type Ndc80 under the control of the Gal1 promoter in the background of *ndc80-14D* and, thus, was unable to grow when Ndc80 expression was repressed by glucose (Figure 4B). Furthermore, when cells grown in 0.1% galactose to allow Ndc80 expression just above wild-type levels were shifted to glucose, the amount of Ndc80 in these cells dropped to levels undetectable by western analysis (Figure 4C). When released from an α factor arrest after Ndc80 depletion, the *ndc80-14D* mutants arrested as large budded cells (Figure 4D) with a 2N DNA content (Figure 4G) short ($<2\,\mu$m) spindles (Figure 4E) and bipolar attached kinetochores (Figures 4F and 6E). Furthermore, Pds1 levels remained highly stable throughout the *ndc80-14D* arrest (Figure 5A). Thus, these data are consistent with the idea that *ndc80-14D* cells arrest in metaphase due to long-lasting SAC activation. In contrast to this, cells depleted of wild-type Ndc80 in the absence of Ndc80-14D, exhibited 2 h after the release from a G1 arrest long, partially broken spindles (Figure 4E) and predominately kinetochores that did not localize to the spindle (Figure 4F). This shows a severe defect in kinetochore–microtubule attachment. Furthermore, these cells accomplished re-budding (Figure 4D) and DNA re-replication to 4N (Supplementary Figure S2) indicative of cells that fail to maintain SAC activation. Thus, the *ndc80-14D* phenotype is not a consequence of Ndc80 depletion *per se*. Mad2 localization at kinetochores is a hallmark of cells with an activated SAC (see 'Introduction'). To confirm that the *ndc80-14D* mutation results in SAC activation, we therefore investigated Mad2 localization in *ndc80-14D* cells released from an α factor arrest after Ndc80 depletion and compared the results with Mad2 localization in cells released into medium containing nocodazole. About 145 min after the release, 71% of untreated *ndc80-14D* cells, 86% of nocodazole treated *ndc80-14D* cells and 96% of nocodazole treated wild-type cells revealed focal Mad2 signals indicative of kinetochore localization (Figure 5B and C). The remaining cells predominately eluded analysis because of a too high Mad2-3GFP background signal. Notably, 69% of the Mad2

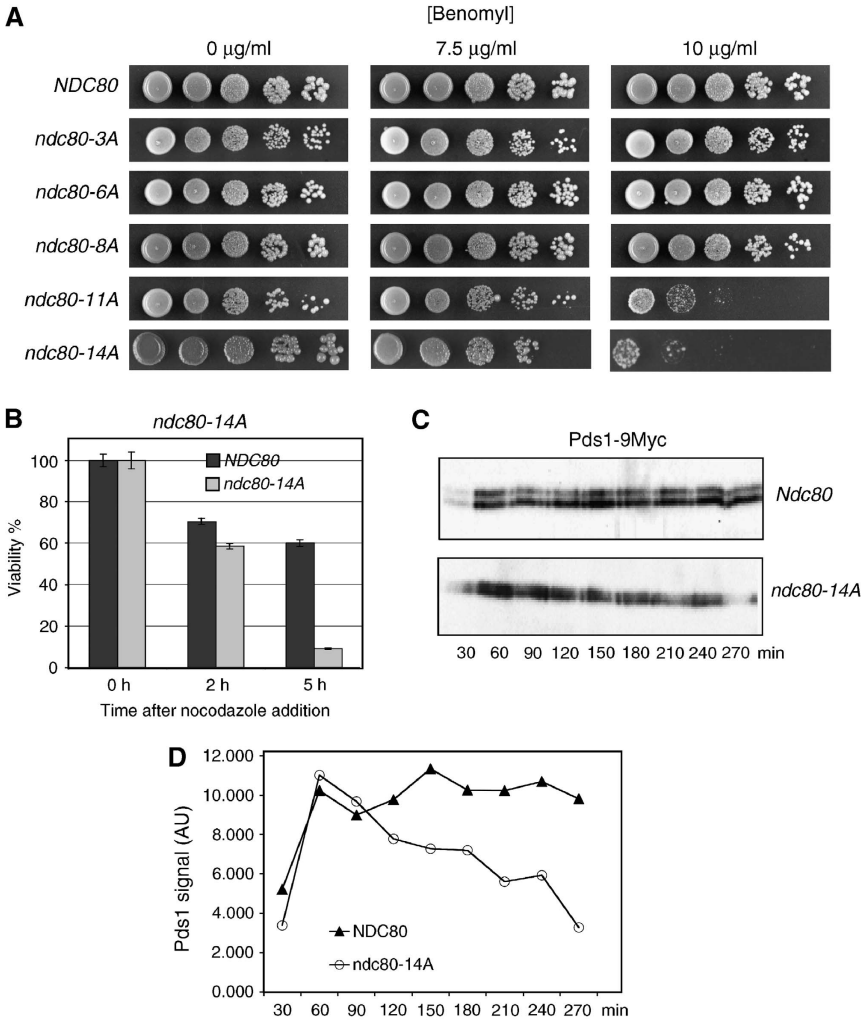

Figure 3 Ndc80 serine and threonine to alanine mutants exhibit a SAC defect. (**A**) *ndc80-11A and ndc80-14A* are benomyl sensitive. Serial dilutions of cells with increasing numbers of phosphorylation sites mutated to alanine (see Table II for exact specification of sites mutated) were tested for growth on YPD plates containing the indicated concentration of benomyl. (**B**) Survival assay. *ndc80-14A* cells were exposed to nocodazole for the indicated times and then plated onto YPD plates lacking the drug. Viability was calculated by normalizing the number of colonies formed by cells treated with nocodazole to the number of colonies formed by untreated cells (0 h). (**C**) *ndc80-14A* fails to maintain long-term Pds1 stability upon nocodazole treatment. α Factor arrested *PDS1-9MYC* cells were released into medium containing nocodazole. For the indicated time points after the release, Pds1 levels in whole cell extracts were determined by western analysis using anti-Myc antibody. (**D**) Quantification of (C). AU, arbitrary units.

signals in untreated *ndc80-14D* cells were observed in two lobes most likely reflecting clusters of sister kinetochores in metaphase, whereas 73 or 80% of the Mad2 signals in the nocodazole-treated cells were observed as one cluster reflecting the fact that sister kinetochores remain in close proximity in the absence of microtubules. Furthermore, the average signal intensity of Mad2-3GFP in untreated *ndc80-14D* cells was similar to that of nocodazole-treated cells (Figure 5D), indicating that the *ndc80-14D* mutation promotes the efficient binding of Mad2 to the majority of kinetochores within a cell. In summary, we therefore conclude that simulating constitutive Ndc80 phosphorylation, as in *ndc80-14D*, results in constitutive SAC activation.

ndc80-14D kinetochores support stable bipolar microtubule interaction

SAC activation can be a result of defect kinetochores if the defect interferes with kinetochore–microtubule interaction but still allows kinetochore-dependent SAC signalling. As positively charged amino acids (lysines) residing in the N-terminal domains of human Ndc80 and Nuf2 are important for *in vitro* interaction between the human Ndc80 complex and microtubules (Ciferri *et al*, 2008), the introduction of 14 negative charges might severely affect kinetochore–microtubule interaction in *ndc80-14D* cells. Therefore, we tested the functionality of Ndc80-14D. Cellular levels of Ndc80-14D were very similar to wild-type Ndc80 levels (not shown), demonstrating that the mutations did not produce an unstable protein. Furthermore, Ndc80-14D clearly is assembled into kinetochores in the presence (Figure 6A) or absence (Figure 6B) of wild-type Ndc80. Next, we analysed *in vitro* microtubule binding of purified $Ndc80^{1-257}$ and $Ndc80^{1-257}$-14D. As shown in Figure 6C and D, at high tubulin to $Ndc80^{1-257}$ ratios, the N-terminal domains of Ndc80 and $Ndc80^{1-257}$-14D interact with microtubules *in vitro* (even in the absence of Nuf2) with similar efficiency. When

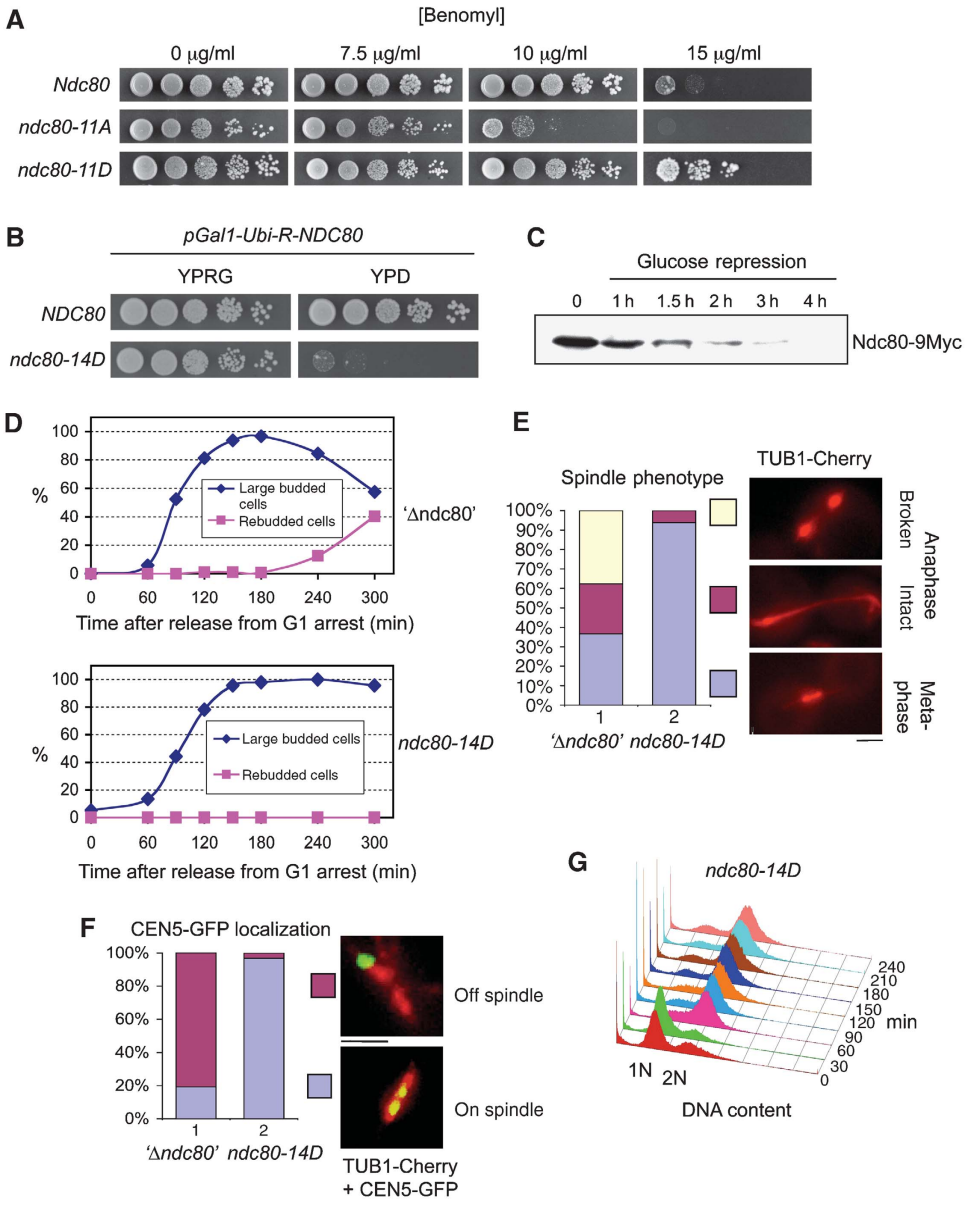

Figure 4 Phenotype of Ndc80 serine and threonine to aspartate mutants. (**A**) *ndc80-11D* is hypertolerant to benomyl. Serial dilutions of cells were tested for growth on YPD plates containing the indicated concentrations of benomyl. (**B–F**) *ndc80-14D* arrests in metaphase. (B) Serial dilutions of strain YSK1173 (*ndc80-14D; PGAL1-Ubi-R-NDC80-9Myc; TUB1-Cherry; CEN5-GFP*) and YSK1128 (*NDC80; PGAL1-Ubi-R-NDC80-9myc*) were tested on YPRG (2% raffinose, 0.1% galactose) or YPD (2% glucose) plates for growth. (C) Ndc80 depletion. Strain YSK1173 was grown to mid-log phase in raffinose medium supplemented with 0.1% galactose. The medium was exchanged for YPD (time point 0), whole cell extracts were derived at the indicated time points and subjected to western analysis with anti-Myc antibody. (D–G) YSK1173 and YSK1155 (*PGAL1-Ubi-R-NDC80-9Myc; TUB1-Cherry; CEN5-GFP*) ('Δ*ndc80*') were synchronized by α factor treatment in YPD for 3 h and released into YPD medium. (D) Cells with large buds (>2/3 of mother) and cells that exhibited rebudding were counted at the indicated time points ($n > 100$). (E) Spindles were visualized 120 min after the release by fluorescent microscopy (TUB1-Cherry) and quantified as indicated ($n > 100$). Bar: 2 μm. (F) Spindles (TUB1-Cherry) and kinetochores of chromosome V (CEN5-GFP) were visualized 120 min after the release by fluorescent microscopy and quantified as indicated. Bar: 2 μm. (**G**) The DNA content of YSK1173 was determined by FACS analysis at the indicated time points after the release. α Factor was re-added to the cultures 1 h after the release to arrest cells that executed mitosis in G1 of the next cell cycle. For FACS, data concerning YSK1173 and YSK1155 in the absence of α factor see Supplementary Figure S2.

approaching saturation (at low tubulin to Ndc80$^{1-257}$ ratios), the binding of Ndc80$^{1-257}$-14D was about 1.5-fold less efficient than the wild type (Figure 6D). The *in vitro* interaction assay predominantly monitors lateral microtubule attachment. *In vivo*, however, kinetochores finally achieve a bipolar end on attachment that has to withstand the force generated under this condition. As this force distances sister kinetochores from one another (Goshima and Yanagida, 2000) the separation of sister kinetochores at metaphase is a readout for the stability of kinetochore–microtubule attachment *in vivo*. Sister kinetochore separation and rejoining is a dynamic process (kinetochore breathing). At a given time point about 2/3 of the sister kinetochores appear separated when wild-type cells are arrested in metaphase by depletion of the APC activator Cdc20 (Figure 6E). As mentioned earlier, exposing the *ndc80-14D* mutation also results in a metaphase arrest.

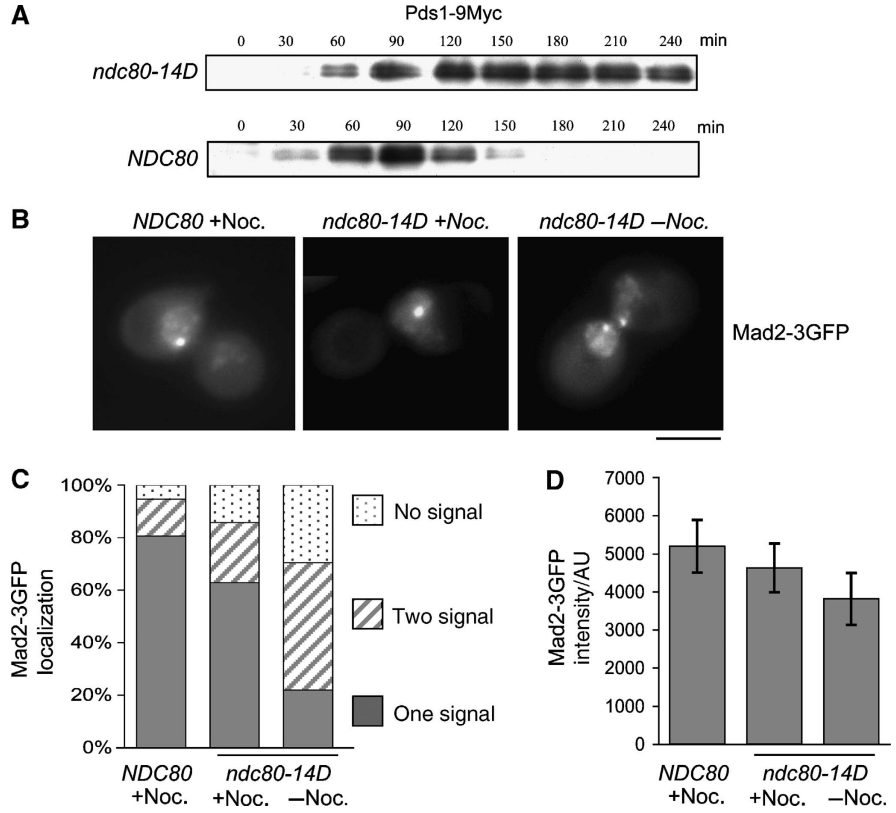

Figure 5 SAC activation causes the *ndc80-14D* arrest in metaphase. (**A**–**D**) Cells were synchronized by α factor treatment and depleted of Ndc80 as in Figure 4D–F. (A) Pds1 levels. At the indicated time points after the release, whole cell extracts of strains YSK1173 (*ndc80-14D; PGAL1-Ubi-R-NDC80; PDS1-9MYC)* and YSK1128 (*NDC80; PGAL1-Ubi-R-NDC80; PDS1-9MYC*) were obtained. Pds1 levels were determined by western analysis using anti-Myc antibody. (B) Mad2 localization. Strains YSK1226 (*ndc80-14D; PGAL1-Ubi-R-NDC80; MAD2-3GFP*) and YMS739 (*NDC80*; *MAD2-3GFP*) were analysed by fluorescence microscopy 145 min after the release into YPD with or without nocodazole (Noc.) as indicated. Bar: 5 μm. (C) Quantification of Mad2-3GFP localization. $n > 100$ for each sample. (D) Quantification of Mad2-3GFP signal intensity. The data represent the intensity average of 60 cells (for each sample). When two signals per cell were detected, the values were combined. Error bars represent the standard deviation of the measurements. AU, arbitrary units.

When kinetochore breathing was analysed in these cells, the percentage of separated sister kinetochores was indistinguishable from that in wild-type cells arrested by Cdc20 depletion (Figure 6E). Thus, the interaction of *ndc80-14D* kinetochores and microtubules is stable enough to allow wild-type-like bipolar attachment. To support this, we investigated the kinetochore localization of Dam1, a component of the Dam1 complex, that is dependent on kinetochore–microtubule interaction and thus on a functional Ndc80 complex (Janke *et al*, 2002; Li *et al*, 2002) by ChIP. Whereas Ndc80 depletion *per se* resulted in a severe Dam1 localization defect no such effect was observed for *ndc80-14D* within the error range of the experiment (Figure 6F). In summary, we therefore conclude that *ndc80-14D* kinetochores maintain an active SAC even when they have achieved bipolar attachment, the cellular prerequisite for SAC inactivation.

Elimination of SAC signalling rescues the ndc80-14D defect

If simulating constitutive phosphorylation of the Ndc80 N-terminal domain maintains SAC activation, irrespective of the fact that mitotic events have progressed to a state that permits and requires SAC inactivation, then the *ndc80-14D* mutant would be inviable as a result of aberrant SAC activation and not because of kinetochore defects that affect kinetochore–spindle interaction. To test this hypothesis, we eliminated SAC signalling in the *ndc80-14D* mutant by disrupting *MAD2* or *BUB1* and tested for cell growth. As mentioned earlier, the *ndc80-14D* mutant is inviable (as revealed by counter selecting against a plasmid-based wild-type copy of NDC80 with FOA). In contrast to this, Δ*mad2*, *ndc80-14D* or Δ*bub1*, *ndc80-14D* double mutants were viable (Figure 7A) and conversely, re-introduction of either *MAD2* or *BUB1* into the respective double mutant resulted in nonviable cells. For unknown reasons, the double mutants grew slower than Δ*mad2* and Δ*bub1* cells in liquid media (doubling time of 115 versus 90 min at logarithmic growth). Importantly, however, the loss rate of an artificial chromosomal fragment (see Materials and methods) in the Δ*bub1*, *ndc80-14D* double mutant (7.2×10^{-3} per cell division) and in Δ*bub1* cells (9.1×10^{-3} per cell division) was very similar. Furthermore, double mutants and Δ*mad2* cells exhibited the same sensitivity towards benomyl (Figure 7B). Thus, *ndc80-14D* kinetochores function reliably once SAC signalling is eliminated. To our knowledge, there is currently no case known where a lethal kinetochore mutation can be rescued by eliminating SAC. In the contrary, disrupting SAC components in viable kinetochore mutants is frequently synthetic lethal. Therefore, we conclude that disruption of *MAD2* or *BUB1* in the *ndc80-14D* mutant allows the cells to circumvent an aberrant SAC induced cell-cycle arrest and let them perform sufficiently reliable chromosome segregation. Taken together, our data

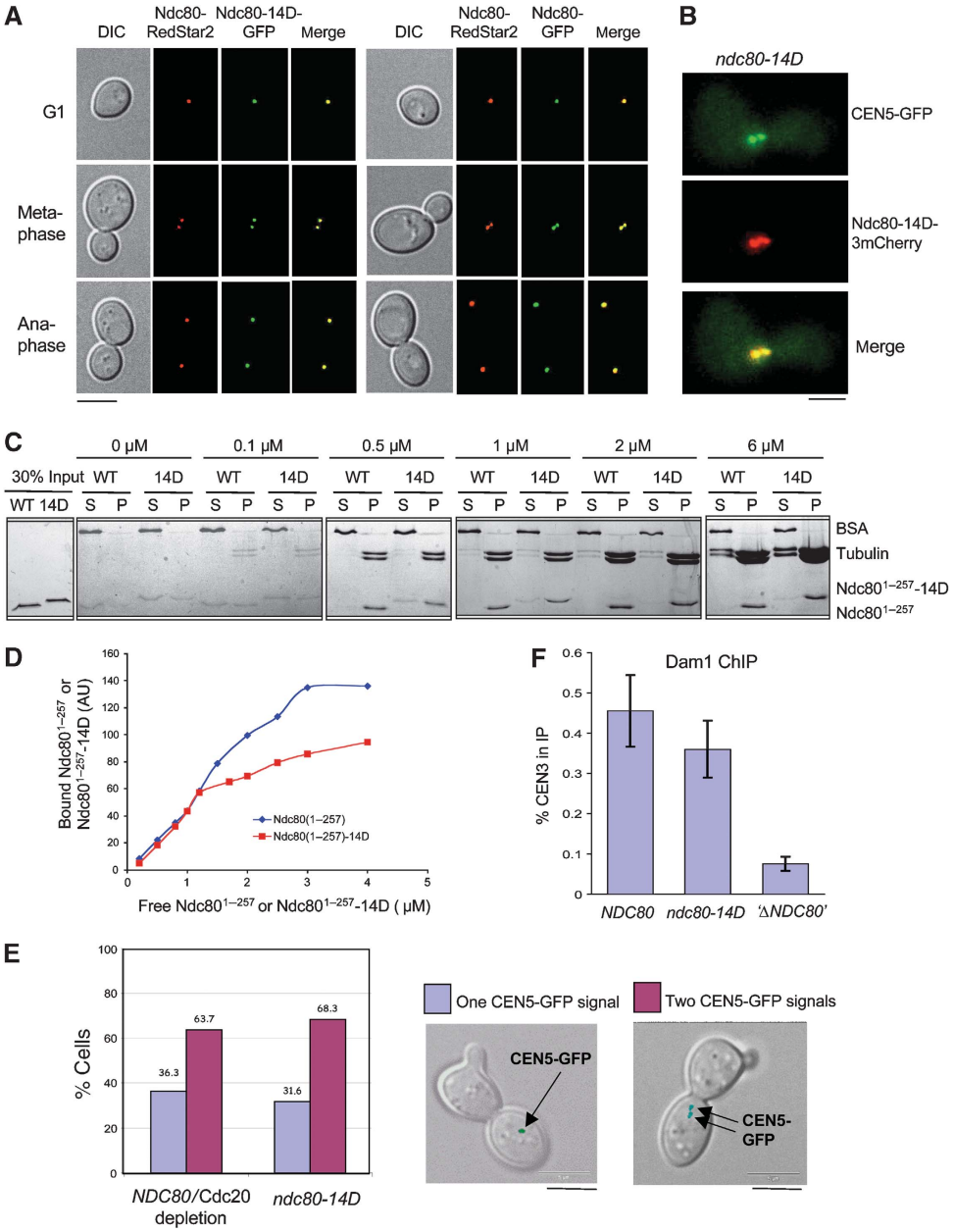

Figure 6 *ndc80-14D* kinetochores are functional. (**A**, **B**) Kinetochore localization of Ndc80-14D. (A) Strain YSK1106 (*NDC80-RedStar2; NDC80-GFP*) and strain YSK1124 (*NDC80-RedStar2; ndc80-14D-GFP*) were grown to mid-log phase and analysed by fluorescence microscopy. Bar: 5 µm. (B) Strain YMK1319 (*ndc80-14D-Cherry*; *PGAL1-Ubi-R-NDC80-9Myc;* , *TetO*::*CEN5*, *TetR-GFP*) was depleted of Ndc80 and synchronized by α factor treatment in YPD for 3 h. Cells were analysed 120 min after the release into YPD by fluorescence microscopy. CEN5-GFP marks kinetochore localization. Bar: 2 µm. (**C**, **D**) Ndc80$^{1-257}$-14D binds to microtubules *in vitro*. (C) Taxol-stabilized microtubules at the indicated tubulin dimer concentrations were incubated with purified 1 µM His10-Ndc80$^{1-257}$ (WT) and His10-Ndc80$^{1-257}$-14D (14D) and subsequently centrifuged. About 30% of the pellet (P) and 10% of the supernatant (S) were analysed by SDS–PAGE and Coomassie staining. BSA served as a negative-binding control. (D) His10-Ndc80$^{1-257}$ and His10-Ndc80$^{1-257}$-14D at the indicated concentrations were incubated with or without taxol-stabilized microtubules at 1 µM Tubulin dimer concentration. After centrifugation, 30% of the pellets were subjected to SDS–PAGE plus Coomassie staining and the His10-Ndc80$^{1-257}$ or His10-Ndc80$^{1-257}$-14D bands were quantified. The values for bound His10-Ndc80$^{1-257}$ or His10-Ndc80$^{1-257}$-14D shown in the graph represent the pelleted amount in the presence of microtubules minus the pelleted amount in the absence of microtubules. AU, arbitrary units. (**E**) *ndc80-14D* cells exhibit wild-type-like bipolar attachment. Strains YMS412 (*NDC80, pGAL-CDC20, TetO*::*CEN5, TetR-GFP*) and YSK1173 (*ndc80-14D, pGAL-Ubi-R-NDC80, TetO*::*CEN5, TetR-GFP*) were synchronized as in (B). CEN5-GFP was visualized by fluorescence microscopy 120 min after the release. The percentage of cells with one or two CEN5-GFP signals (as shown by DIC/GFP overlays) was quantified ($n > 100$). Bar: 5 µm. (**F**) Dam1 localization at *ndc80-14D* kinetochores. Strain YSK1170 (*ndc80-14D*; *PGAL1-Ubi-R-NDC80-9myc*), strain YMS412 (*NDC80, PGAL1-CDC20*) and strain YSK1155 (*PGAL1-Ubi-R-NDC80-9Myc*) ('Δndc80') were synchronized by α factor treatment in YPD for 3 h and released into YPD. Cells were subjected to ChIP analysis with anti-Dam1 antibody 120 min after the release. The percentage of CEN3 DNA recovered in the IP is shown in respect to the input. Error bars represent the standard deviation of two independent experiments. Note that under these conditions, YMS412 arrests in metaphase (due to Cdc20 depletion) and, thus, provides the appropriate control for YSK1170 that arrests in metaphase due to the *ndc80-14D* mutation.

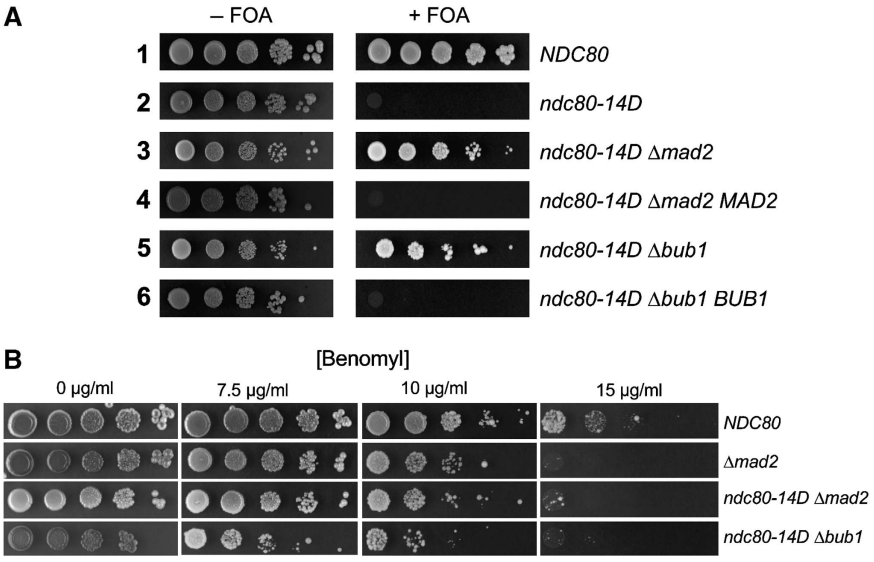

Figure 7 Elimination of SAC signalling rescues ndc80-14D cells. (**A**) Deletion of *MAD2* or *BUB1* rescues *ndc80-14D* mutants. All strains harboured an episomal copy of *NDC80* on a *CEN/URA3* plasmid. Δ*mad2 MAD2* or Δ*bub1 BUB1* cells harboured the wild-type gene copy on a *CEN/LEU2* plasmid. All other strains harboured an empty *CEN/LEU2* plasmid. Serial dilutions of cells were tested for growth on plates lacking leucine in the absence or presence of FOA. FOA counter selects for the plasmid-based copy of *NDC80*. (**B**) Serial dilutions of cells with the specified genotype were tested for growth on YPD plates containing the indicated concentrations of benomyl.

suggest that phosphorylation of the Ndc80 N-terminal domain, putatively dependent on Mps1, is required and sufficient to promote SAC activation.

Role of Ipl1 phosphorylation sites

Ipl1-dependent phosphorylation of kinetochore proteins is considered to weaken nonbipolar kinetochore–microtubule interactions (Biggins and Murray, 2001; Tanaka *et al*, 2002). Also, phosphorylation by Aurora B kinase/Ipl1 has been reported to weaken the interaction between human (Ciferri *et al*, 2008) or *Caenorhabditis elegans* (Cheeseman *et al*, 2006) Ndc80 complexes and microtubules *in vitro*. Therefore, we wondered how mimicking phosphorylation at Ipl1 sites would correlate/contribute to the ndc80-14D phenotype. Cells that had only the three Ipl1 sites of Ndc80 (T54, T74, S100) mutated to aspartate (*ndc80-3D*, Supplementary Table SI) grew like wild-type cells indicating that Ipl1 phosphorylation is not sufficient to produce the ndc80-14D effect. Changing the one mutated Ipl1 site in *ndc80-14D* (T74D) back to wild type produced inviable cells (ndc80-13D, Supplementary Table SI) that could be rescued by *MAD2* deletion (not shown). Thus, they behaved like *ndc80-14D* in this respect, indicating that mimicking phosphorylation at Ipl1 sites is not essential for the ndc80-14D phenotype. Finally, *ndc80-14D*** (Supplementary Table SI) a strain that is identical to *ndc80-14D* with the exception that it carries T54D plus S100D instead of T79D plus T82D (and thus has all three Ipl1 sites mutated) was inviable but could be rescued by *MAD2* depletion (not shown), indicating that Ipl1 and Mps1 phosphorylation of Ndc80 might function additively in SAC activation.

All aspartate mutants analysed (Supplementary Table SI) harbouring a subset of the *ndc80-13D* mutations were viable. Thus, it appears that introducing a certain quantity of negative charge is an essential factor in establishing the *ndc80-14D* phenotype. On the other hand, some mutations appear to contribute more than others to the phenotype. *ndc80-14D** (Supplementary Table SI) that carries 14 aspartate mutations, like *ndc80-14D*, but harbours mutations at positions 54, 56 and 58 instead of mutations at positions 74, 79 and 82 was viable.

Mps1 function is also required downstream of Ndc80 phosphorylation

Mps1 overexpression results in Ndc80 hyperphosphorylation and in constitutive SAC activation. If this is the sole function of Mps1 in SAC signalling, SAC activation should occur independent of Mps1 in the *ndc80-14D* mutant. To test this possibility, we constructed an *ndc80-14D* strain that allowed simultaneous depletion of a wild-type Ndc80 as well as Mps1. Mps1 is required for spindle pole body assembly as well as SAC function. In order not to interfere with spindle pole body duplication, we first arrested the cells by hydroxy urea (when spindle pole body duplication is completed) before we depleted Ndc80 and Mps1. Then we released them from the arrest into nocodazole media. Nocodazole treatment produces a SAC- dependent cell-cycle arrest if Mps1 is present. Consistent with Mps1's essential SAC function, Mps1-depleted *NDC80* cells did not arrest, as revealed by DNA re-replication to 4N and re-budding (Supplementary Figure S3, not shown). Mps1-depleted *ndc80-14D* cells also re-replicated their DNA and re-budded, indistinguishable from wild-type cells. Thus, the SAC defect caused by the absence of Mps1 cannot be compensated by an *ndc80-14D* kinetochore. Consequently, Mps1 function is also required downstream of Ndc80 phosphorylation for SAC signalling.

Discussion

Mps1-dependent phosphorylation of Ndc80

We found that Mps1 phosphorylates Ndc80 *in vitro* and promotes Ndc80 phosphorylation *in vivo*. Upon *in vitro* phosphorylation, 25 phosphorylated serine/threonine residues, that is about half the available sites, were identified

within the Ndc80 N-terminal domain ($Ndc80^{1-257}$). Similar to published Mps1 phosphorylation data (for example, Shimogawa *et al*, 2006; Jelluma *et al*, 2008), no Mps1 consensus site could be deduced from the Ndc80 phosphorylation sites. This indicates that the active centre of Mps1 accepts a broad variety of amino-acid sequences. On the other side, Mps1 phosphorylated Ndc80 preferentially over Nuf2, Spc24 and Spc25, when the Ndc80 complex was provided as a substrate. Mps1 also interacts with $Ndc80^{1-257}$ *in vitro*. Although it is currently unclear which Mps1 region is involved, the interaction of Ndc80 with Mps1 sequences other than the active centre can be one explanation for the observed substrate selectivity. A second explanation may be related to the fact that 18 of the identified phosphorylation sites reside in the unstructured N-terminal tail of *S. cerevisiae* Ndc80 (Supplementary Figure SI). Nuf2, Spc24 and Spc25 lack long unstructured terminal tails and, therefore, may be weaker Mps1 substrates.

Ndc80 phosphorylation and SAC activation

Several lines of evidence support that Mps1-dependent phosphorylation of Ndc80 is an integral step in SAC activation. (1) Changing 11 or 14 Ndc80 phosphorylation sites to alanine as in *ndc80-11A* or *ndc80-14A* resulted in sensitivity to microtubule destabilizing drugs. Furthermore, nocodazole treated *ndc80-14A* failed to maintain high Pds1 levels over the period of time that nocodazole treated wild-type cells do. These data are in agreement with the concept that interfering with Ndc80 phosphorylation at the targeted sites compromises SAC function. Although the Pds1 degradation kinetics of nocodazole treated *ndc80-14A* cells does not resemble that of wild-type cells, it is also not equivalent to that of Δ*mad2* mutants where SAC is completely abolished (unpublished data), indicating that *ndc80-14A* has residual SAC activity. However, only about half of the identified Mps1 phosphorylation sites are eliminated in this strain and many possible mutant variations have not been analysed. Particularly, mutating more than 14 phosphorylation sites to alanine might exhibit a stronger phenotype than *ndc80-11A* and *ndc80-14A*. Furthermore, Mps1-dependent phosphorylation of kinetochore proteins in the vicinity of Ndc80 (such as Nuf2) might contribute to SAC activation. (2) Changing the sites mutated in *ndc80-11A* to aspartate produced cells (*ndc80-11D*) that exhibit higher benomyl tolerance than wild-type cells. This is in agreement with the idea that *ndc80-11D* is better fitted to cope with a microtubule poison due to a particularly robust SAC activation. (3) *ndc80-14D*, in contrast to the equivalent alanine mutant *ndc80-14A* is inviable. Upon depletion of a background wild-type copy, *ndc80-14D* arrests as large budded cells with a short metaphase spindle and a 2N DNA content. (4) *ndc80-14D* kinetochores achieve wild-type-like bipolar attachments. Despite this, *ndc80-14D* cells maintain high Pds1 levels and exhibit significant amounts of Mad2 at the two clusters of kinetochores that are the result of bipolar kinetochore attachment. This is reminiscent of the Bub3 kinetochore localization in cells that overexpress Mps1 (Kerscher *et al*, 2003). (5) Most importantly *ndc80-14D* cells can be rescued by disruption of SAC signalling. This is in agreement with constitutive SAC activation in *ndc80-14D* and may reflect cell lethality and rescue respectively upon Mps1 overexpression in wild-type and Δ*mad2* strains (Hardwick *et al*, 1996).

Kinetochore function in ndc80-14D cells

Mps1 is known to regulate kinetochore bi-orientation (Maure *et al*, 2007) and kinetochore positioning to microtubule plus ends through Dam1 phosphorylation (Shimogawa *et al*, 2006). Furthermore, as mentioned earlier, the introduction of negative charge into the Ndc80 N-terminal domain as in *ndc80-14D* might disrupt kinetochore–microtubule attachment, and this would consequently activate SAC *per se*.

Several lines of evidence support that ndc80-14D kinetochores are functional and in particular that kinetochore–microtubule interaction is not severely affected. (1) $Ndc80^{1-257}$-14D binds to microtubules *in vitro*. In comparison to wild-type $Ndc80^{1-257}$, the binding efficiency only decreased (by a factor of 1.5) when the $Ndc80^{1-257}$-14D concentration approached the tubulin dimer concentration in the assay. The reason for this is unclear, but it is questionable whether this reflects a physiological situation. (2) *In vivo*, *ndc80-14D* cells arrest with bipolar attached kinetochores experiencing tension indistinguishable from wild-type cells that have been arrested in metaphase by APC inactivation. (3) Dam1, a subunit of the Dam1 complex localizes efficiently to *ndc80-14D* kinetochores. This indicates proficient kinetochore–microtubule interaction as kinetochore localization of the Dam1 complex depends on Ndc80 and on kinetochore–microtubule interaction. (4) The kinetochore–microtubule attachment in *ndc80-14D* cells suffices to support cell viability and reliable chromosome segregation when SAC signalling is disrupted.

The apparent discrepancy that the *in vitro* interaction between the Ndc80 complex and microtubules is affected by altering the charge or Ipl1-dependent phosphorylation state of the metazoan Ndc80 and Nuf2 N-terminal domains (see above), whereas Ndc80-14D exhibits no strong interaction defect and performs satisfactory *in vivo* could be explained in several ways. (1) Phosphorylating Ndc80 (by Ipl1) may not be the principal step to regulate kinetochore–microtubule interaction in *S. cerevisiae*. Instead, phosphorylating components of the Dam1 complex, that has no counterpart in higher eukaryotes, may fulfill this function in *S. cerevisiae* (Cheeseman *et al*, 2002). Consistent with this assumption is that mimicking phosphorylation at the three Ipl1 phosphorylation sites of Ndc80 has no affect on cell growth in *S. cerevisiae*. (2) Phosphorylation of Ndc80 might resolve syntelic or merotelic kinetochore–microtubules attachments but allow bipolar attachments when kinetochore–microtubule interaction is sustained by the applied tension. (3) A binding defect observed *in vitro* might be attenuated *in vivo* through the action of unaltered Nuf2. Interestingly, yeast cells that solely express a truncated Ndc80 that lacks amino acids 1–116 grow like wild-type cells (Supplementary Figure S4), although the N-terminal tail of Ndc80, as shown for the human homologue (Wei *et al*, 2007), is important for microtubule binding *in vitro*. Alternatively, the principals postulated for the interaction of the metazoan Ndc80/Nuf2 heterodimer with microtubules might be altered in *S. cerevisiae*.

Models for the role of Mps1-dependent phosphorylation of Ndc80 in SAC activation

Taken together, our data indicate that the requirements for SAC inactivation have been satisfied in metaphase arrested *ndc80-14D* cells but despite this, *ndc80-14D* kinetochores create a strong SAC signal. Therefore, we postulate that

Mps1-dependent phosphorylation of Ndc80 is important for SAC activation possibly by introducing negative charge into the N-terminal domain and removal of these phosphate residues is required to inactivate SAC. There are several possibilities (that are not exclusive) how this might be orchestrated (Supplementary Figure S5). Mps1 might recognize Ndc80 only at kinetochores lacking bipolar attachment. Once Mps1 has left the bipolar attached kinetochore, a constitutively active phosphatase would dephosphorylate Ndc80 (Supplementary Figure S5A). This may be in agreement with the observed kinetochore localization of Mps1. Conversely, Mps1 might constitutively phosphorylate free or kinetochore Ndc80 but only Ndc80 at a bipolar attached kinetochore would be recognized by a phosphatase counteracting Mps1 activity (Supplementary Figure S5B). Finally, Ndc80 might predominantly get phosphorylated off the kinetochore and dephosphorylated at the kinetochore. A rapid exchange of Ndc80 at the kinetochore before metaphase might guarantee that there is sufficient phosphorylated Ndc80 at the kinetochore to activate the SAC. Upon bipolar attachment, the exchange rate of kinetochore proteins including Ndc80 significantly drops (Joglekar *et al*, 2006), which would lead to predominantly dephosphorylated Ndc80 at the kinetochore (Supplementary Figure S5C). Furthermore, Mps1 is inactivated by APC in anaphase (Palframan *et al*, 2006).

ndc80-14D kinetochores do not promote SAC activation in the absence of Mps1. This might raise the question whether Mps1's role in SAC signalling involves Ndc80 phosphorylation. On the other hand, it is quite possible that Mps1 performs at least one more signalling step downstream of Ndc80 phosphorylation. Hyperphosphorylation of Mad1 has been described upon Mps1 overexpression (Hardwick *et al*, 1996) and thus could be this step. Having SAC functions downstream of Ndc80 phosphorylation might also be the reason why Mps1 overexpression still leads to SAC activation in *ndc10-1* cells (Fraschini *et al*, 2001) that presumably lack any kinetochores. Alternatively, Mps1 overexpression might restore SAC signalling from few partially functional kinetochores left in these cells.

The observation that the presence of specific phosphoepitopes (3F3/2) correlates with the absence of tension at the kinetochore exists for quite a time (Nicklas *et al*, 1995). Recently, it was reported that polo kinase is responsible for these phosphorylation events in vertebrate cells (Ahonen *et al*, 2005). In *S. cerevisiae*, the existence of kinetochore-based 3F3/2 epitopes has not been described. Also, no role in SAC activation is currently known for polo kinase in *S. cerevisiae*. In agreement with this, the Ndc80 phosphorylation sites identified here do not fit the 3F3/2 or polo kinase motif (Nakajima *et al*, 2003). It will be of interest whether Mps1-dependent phosphorylation of Ndc80 occurs in vertebrates. Otherwise, it might represent an alternative strategy of *S. cerevisiae* to label nonbipolar attached kinetochores by phosphate groups equivalent to the establishment of 3F3/2 phosphoepitopes or the Aurora B/Ipl1 phosphorylation events in higher eukaryotes.

Materials and methods

Mps1 kinase assay

Recombinant 10His-Ndc80$^{1-257}$ (about 1.25 pmol) or tandem affinity purified Ndc80 complex (about 1.9 pmol Ndc80) were incubated with tandem affinity purified Mps1 (1.2 pmol), 10 μCi [γ-^{32}P]-ATP (specific activity: 3000 Ci/mmol) and 10 μM cold ATP in 80 μl kinase assay buffer (50 mM Tris–HCl 7.5, 10 mM $MgCl_2$, 100 mM NaCl, 0.5 mM DTT, 1 mM PMSF) at 30°C for 60 min. Reactions were terminated by the addition of 10% TCA (final concentration) on ice and the precipitate was subjected to SDS–PAGE. The incorporation of ^{32}P was visualized using a phosphorimager and the QuantityOne software from Biorad. For the identification of phosphorylation sites by mass spectrometry, about 25 pmol 10His-Ndc80$^{1-257}$ was incubated with 1.2 pmol Mps1 in kinase assay buffer containing 10 mM ATP at 30°C for 2 h.

Supplementary data

Supplementary data are available at *The EMBO Journal* Online (http://www.embojournal.org).

Acknowledgements

We thank Eileen Dietzel, Petra Ihrig and Jürgen Reichert for excellent technical assistance, Carsten Jäger for work regarding Mps1 and Ndc80 complex co-purification and Sue Biggins for providing plasmids. This work was supported by a grant from the Deutsche Forschungsgemeinschaft.

References

Ahonen LJ, Kallio MJ, Daum JR, Bolton M, Manke IA, Yaffe MB, Stukenberg PT, Gorbsky GJ (2005) Polo-like kinase 1 creates the tension-sensing 3F3/2 phosphoepitope and modulates the association of spindle-checkpoint proteins at kinetochores. *Curr Biol* **15:** 1078–1089

Biggins S, Murray AW (2001) The budding yeast protein kinase Ipl1/Aurora allows the absence of tension to activate the spindle checkpoint. *Genes Dev* **15:** 3118–3129

Castillo AR, Meehl JB, Morgan G, Schutz-Geschwender A, Winey M (2002) The yeast protein kinase Mps1p is required for assembly of the integral spindle pole body component Spc42p. *J Cell Biol* **156:** 453–465

Chan GK, Liu ST, Yen TJ (2005) Kinetochore structure and function. *Trends Cell Biol* **15:** 589–598

Cheeseman IM, Anderson S, Jwa M, Green EM, Kang J, Yates III JR, Chan CS, Drubin DG, Barnes G (2002) Phospho-regulation of kinetochore-microtubule attachments by the Aurora kinase Ipl1p. *Cell* **111:** 163–172

Cheeseman IM, Chappie JS, Wilson-Kubalek EM, Desai A (2006) The conserved KMN network constitutes the core microtubule-binding site of the kinetochore. *Cell* **127:** 983–997

Ciferri C, De Luca J, Monzani S, Ferrari KJ, Ristic D, Wyman C, Stark H, Kilmartin J, Salmon ED, Musacchio A (2005) Architecture of the human ndc80-hec1 complex, a critical constituent of the outer kinetochore. *J Biol Chem* **280:** 29088–29095

Ciferri C, Pasqualato S, Screpanti E, Varetti G, Santaguida S, Dos Reis G, Maiolica A, Polka J, De Luca JG, De Wulf P, Salek M, Rappsilber J, Moores CA, Salmon ED, Musacchio A (2008) Implications for kinetochore-microtubule attachment from the structure of an engineered Ndc80 complex. *Cell* **133:** 427–439

DeLuca JG, Gall WE, Ciferri C, Cimini D, Musacchio A, Salmon ED (2006) Kinetochore microtubule dynamics and attachment stability are regulated by Hec1. *Cell* **127:** 969–982

DeLuca JG, Howell BJ, Canman JC, Hickey JM, Fang G, Salmon ED (2003) Nuf2 and Hec1 are required for retention of the checkpoint proteins Mad1 and Mad2 to kinetochores. *Curr Biol* **13:** 2103–2109

Fraschini R, Beretta A, Lucchini G, Piatti S (2001) Role of the kinetochore protein Ndc10 in mitotic checkpoint activation in Saccharomyces cerevisiae. *Mol Genet Genomics* **266:** 115–125

Gillett ES, Espelin CW, Sorger PK (2004) Spindle checkpoint proteins and chromosome-microtubule attachment in budding yeast. *J Cell Biol* **164:** 535–546

Goshima G, Yanagida M (2000) Establishing biorientation occurs with precocious separation of the sister kinetochores, but not the arms, in the early spindle of budding yeast. *Cell* **100:** 619–633

Hardwick KG, Weiss E, Luca FC, Winey M, Murray AW (1996) Activation of the budding yeast spindle assembly checkpoint without mitotic spindle disruption. *Science* **273:** 953–956

Janke C, Ortiz J, Lechner J, Shevchenko A, Magiera MM, Schramm C, Schiebel E (2001) The budding yeast proteins Spc24p and Spc25p interact with Ndc80p and Nuf2p at the kinetochore and are important for kinetochore clustering and checkpoint control. *EMBO J* **20:** 777–791

Janke C, Ortiz J, Tanaka TU, Lechner J, Schiebel E (2002) Four new subunits of the Dam1–Duo1 complex reveal novel functions in sister kinetochore biorientation. *EMBO J* **21:** 181–193

Jelluma N, Brenkman AB, van den Broek NJ, Cruijsen CW, van Osch MH, Lens SM, Medema RH, Kops GJ (2008) Mps1 phosphorylates Borealin to control Aurora B activity and chromosome alignment. *Cell* **132:** 233–246

Joglekar AP, Bouck DC, Molk JN, Bloom KS, Salmon ED (2006) Molecular architecture of a kinetochore-microtubule attachment site. *Nat Cell Biol* **8:** 581–585

Jones MH, Huneycutt BJ, Pearson CG, Zhang C, Morgan G, Shokat K, Bloom K, Winey M (2005) Chemical genetics reveals a role for Mps1 kinase in kinetochore attachment during mitosis. *Curr Biol* **15:** 160–165

Kerscher O, Crotti LB, Basrai MA (2003) Recognizing chromosomes in trouble: association of the spindle checkpoint protein Bub3p with altered kinetochores and a unique defective centromere. *Mol Cell Biol* **23:** 6406–6418

Lauze E, Stoelcker B, Luca FC, Weiss E, Schutz AR, Winey M (1995) Yeast spindle pole body duplication gene MPS1 encodes an essential dual specificity protein kinase. *EMBO J* **14:** 1655–1663

Li Y, Bachant J, Alcasabas AA, Wang Y, Qin J, Elledge SJ (2002) The mitotic spindle is required for loading of the DASH complex onto the kinetochore. *Genes Dev* **16:** 183–197

Martin-Lluesma S, Stucke VM, Nigg EA (2002) Role of Hec1 in spindle checkpoint signaling and kinetochore recruitment of Mad1/Mad2. *Science* **297:** 2267–2270

Maure JF, Kitamura E, Tanaka TU (2007) Mps1 kinase promotes sister-kinetochore bi-orientation by a tension-dependent mechanism. *Curr Biol* **17:** 2175–2182

McCleland ML, Gardner RD, Kallio MJ, Daum JR, Gorbsky GJ, Burke DJ, Stukenberg PT (2003) The highly conserved Ndc80 complex is required for kinetochore assembly, chromosome congression, and spindle checkpoint activity. *Genes Dev* **17:** 101–114

Musacchio A, Salmon ED (2007) The spindle-assembly checkpoint in space and time. *Nat Rev Mol Cell Biol* **8:** 379–393

Nakajima H, Toyoshima-Morimoto F, Taniguchi E, Nishida E (2003) Identification of a consensus motif for Plk (Polo-like kinase) phosphorylation reveals Myt1 as a Plk1 substrate. *J Biol Chem* **278:** 25277–25280

Nicklas RB, Ward SC, Gorbsky GJ (1995) Kinetochore chemistry is sensitive to tension and may link mitotic forces to a cell cycle checkpoint. *J Cell Biol* **130:** 929–939

Palframan WJ, Meehl JB, Jaspersen SL, Winey M, Murray AW (2006) Anaphase inactivation of the spindle checkpoint. *Science* **313:** 680–684

Sandall S, Severin F, McLeod IX, Yates III JR, Oegema K, Hyman A, Desai A (2006) A Bir1-Sli15 complex connects centromeres to microtubules and is required to sense kinetochore tension. *Cell* **127:** 1179–1191

Shimogawa MM, Graczyk B, Gardner MK, Francis SE, White EA, Ess M, Molk JN, Ruse C, Niessen S, Yates III JR, Muller EG, Bloom K, Odde DJ, Davis TN (2006) Mps1 phosphorylation of Dam1 couples kinetochores to microtubule plus ends at metaphase. *Curr Biol* **16:** 1489–1501

Tanaka TU, Rachidi N, Janke C, Pereira G, Galova M, Schiebel E, Stark MJ, Nasmyth K (2002) Evidence that the Ipl1-Sli15 (Aurora kinase-INCENP) complex promotes chromosome bi-orientation by altering kinetochore-spindle pole connections. *Cell* **108:** 317–329

Vigneron S, Prieto S, Bernis C, Labbe JC, Castro A, Lorca T (2004) Kinetochore localization of spindle checkpoint proteins: who controls whom? *Mol Biol Cell* **15:** 4584–4596

Wei RR, Al-Bassam J, Harrison SC (2007) The Ndc80/HEC1 complex is a contact point for kinetochore-microtubule attachment. *Nat Struct Mol Biol* **14:** 54–59

Wei RR, Sorger PK, Harrison SC (2005) Molecular organization of the Ndc80 complex, an essential kinetochore component. *Proc Natl Acad Sci USA* **102:** 5363–5367

Weiss E, Winey M (1996) The Saccharomyces cerevisiae spindle pole body duplication gene MPS1 is part of a mitotic checkpoint. *J Cell Biol* **132:** 111–123

Winey M, Goetsch L, Baum P, Byers B (1991) MPS1 and MPS2: novel yeast genes defining distinct steps of spindle pole body duplication. *J Cell Biol* **114:** 745–754

Wong OK, Fang G (2005) Plx1 is the 3F3/2 kinase responsible for targeting spindle checkpoint proteins to kinetochores. *J Cell Biol* **170:** 709–719

